Cubane lanthanoid complexes with tridentate [O, P=O, O] coordination using tris(5-*tert*-butyl-2-hydroxyphenyl)-phosphine oxide ligands: synthesis, characterisation and magnetic behaviour

Patrick Mangundu[a], Curtis C. Ho [a], Richard A. Mole,[b] Marcus Korb[c*], and Rebecca O. Fuller[a*]

[a] School of Natural Sciences – Chemistry, University of Tasmania, Sandy Bay, Tasmania 7005, Australia.
[b] Australian Nuclear Science and Technology Organisation (ANSTO), Australian Centre for Neutron Scattering, New Illawarra Road, Lucas Heights, New South Wales, Australia
[c] School of Molecular Sciences, The University of Western Australia, Crawley, Western Australia 6009 Australia.
* Corresponding authors email: rebecca.fuller@utas.edu.au & marcus.korb@uwa.edu.au

Supporting Information

Table of Contents

I. Experimental

Synthesis of tris(2-hydroxyphenyl)phosphine oxide ($^1LH_3$)

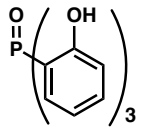

The spectroscopic data is consistent with those reported in reference [2]. ^{1}H NMR (600 MHz, $CDCl_3$): δ 9.43 (s, 3H, OH), 7.47 (m, 3H), 7.01 (m, 6H), 6.91 (m, 3H) ppm. $^{13}C\{^1H\}$ NMR (150 MHz, $CDCl_3$): δ 161.1 (d, $^2J_{C,P}$ = 2.2 Hz), 134.4, 130.9 (d, $J_{C,P}$ = 11.1 Hz), 118.9 (d, $J_{C,P}$ = 13.3 Hz), 117.9 (d, $J_{C,P}$ = 7.7 Hz), 110.3 (d, $^1J_{C,P}$ = 107.3 Hz) ppm. $^{31}P\{^1H\}$ NMR (243 MHz, $CDCl_3$): δ 51.5 ppm.

Synthesis of bis(o-hydroxyphenyl)phenylphosphine oxide ($^2LH_2$)

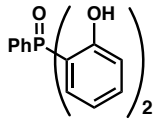

The spectroscopic data is consistent with those reported in reference [3]. ^{1}H NMR (600 MHz, $CDCl_3$): δ 10.35 (s, 2H, OH), 7.62(m, 3H), 7.51 (m, 4H), 7.02 (m, 4H), 6.89 (m, 2H) ppm. $^{13}C\{^1H\}$ NMR (150 MHz, $CDCl_3$): δ 163.6 (d, $J_{C,P}$ = 3.3 Hz), 135.0 (d, $J_{C,P}$ = 2.2 Hz), 133.3 (d, $J_{C,P}$ = 3.3 Hz), 132.0 (m), 131.1, 129.0 (d, $J_{C,P}$ = 12.2 Hz), 119.5 (d, $J_{C,P}$ = 12.2 Hz), 118.9 (d, $J_{C,P}$ = 6.6 Hz), 110.4 (d, $J_{C,P}$ = 105.0 Hz) ppm. $^{31}P\{^1H\}$NMR (243 MHz, $CDCl_3$): δ 48.9 ppm.

Synthesis of tris(4-(tert-butyl)phenyl) phosphate (a)

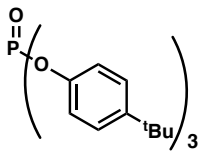

In a round bottom flask, 4-*tert*-butyl phenol (10.00 g, 66.6 mmol) was dissolved in THF and an excess of sodium (2.0 g, 90 mmol) was added. The mixture was refluxed until deprotonation was complete and a further consumption of sodium was no longer visible. The mixture was cooled to room temperature and the remaining sodium was removed using tweezers. The flask was then cooled to 0 °C. Afterwards, $POCl_3$ (2.0 mL, 22.0 mmol) was added and the mixture was stirred. After 16 h, the reaction mixture was poured into ice water. The product was extraction with a diethyl ether / hexane solvent mixture, organic extracts collected and dried over $MgSO_4$. After filtration all solvents were removed from the filtrate and the crude product purified by crystallization from hexane. Yield: 3.59 g (7.26 mmol, 66 %). M = 494.61 g / mol. ^{1}H NMR (400 MHz, $CDCl_3$): 7.34 (dd, $^3J_{H,H}$ = 8.5 Hz, 6H, *m*-C_6H_4), 7.16 (dd, $^3J_{H,H}$ = 8.9 Hz, $^4J_{H,P}$ = 1.1 Hz, 6H, *o*-C_6H_4), δ 1.30 (s, 27H, CH_3) ppm.$^{13}C\{^1H\}$ NMR (101 MHz, $CDCl_3$): δ 148.3 (d, $J_{C,P}$ = 1.4 Hz, ^qC–^{t}Bu), 148.2 (d, $J_{C,P}$ = 7.4 Hz, ^qC–O), 126.6 (d, $J_{C,P}$ = 0.7 Hz, CH), 119.5 (d, $J_{C,P}$ = 4.9 Hz, CH), 34.4 (^qC), 31.4 (CH_3) ppm. $^{31}P\{^1H\}$ NMR (162 MHz, $CDCl_3$): δ –16.9 ppm ppm. Spectroscopic data is consistent with those reported in reference [4].

Synthesis of tris(5-*tert*-butyl-2-hydroxyphenyl)phosphine oxide (LH_3)

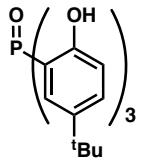

In a Schlenk flask, LDA was prepared by mixing diisopropylamine (11 mL, 77.8 mmol) in THF at –78 °C followed by dropwise addition of MeLi (44 mL, 1.6 M in hexanes, 70.4 mmol). After stirring for 10 minutes, phosphate **a** (3.50 g, 7.08 mmol) was added in one portion, the mixture was allowed to warm to room temperature, and stirring was continued overnight. The mixture was then poured into ice water and neutralized with dilute HCl until a pH value below 5 was reached. The mixture was extracted three times using CH_2Cl_2 and the combined organic extracts dried over $MgSO_4$. In most cases the product did not show impurities and was used directly after removal of solvents. **Yield**: 3.5 g (7.08 mmol, quant). In the case that unreacted starting material or by-products were present, the crude mixture was further purified by column chromatography (silica, 3.5 x 15 cm) using a 95:5 hexane/ethyl acetate solvent mixture. After removal of all volatiles that **LH_3** was obtained as a white solid. M = 494.61 g / mol. Mp: 157.1 °C. ATR-FTIR (ν/cm^{-1}): 3222 w (O–H stretch), 2959 w (C–H asym stretch), 1668 s (C–O stretch). ^{1}H NMR (400 MHz, $CDCl_3$): δ 9.44 (s, 3H, OH), 7.50 (dd, $^3J_{H,H}$ = 8.7, $^5J_{H,H}$ = 2.4 Hz, 3H, H4), 7.08 (dd, $^3J_{H,P}$ = 14.3, $^4J_{H,H}$ = 2.5 Hz, 3H, H6), 6.94 (dd, $^3J_{H,H}$ = 8.7, $^4J_{H,H}$ = 5.6 Hz, 3H, H3), 1.21 (s, 27H, CH_3) ppm. ^{13}C{^{1}H} NMR (101 MHz, $CDCl_3$): δ 160.1 (d, $J_{C,P}$ = 3.1 Hz, ^{q}C–^{t}Bu), 142.3 (d, $J_{C,P}$ = 11.5 Hz, ^{q}C–O), 132.7 (d, $J_{C,P}$ = 2.3 Hz, CH), 127.7 (d, $J_{C,P}$ = 10.5 Hz, CH), 118.6 (d, $J_{C,P}$ = 8.1 Hz, CH), 110.3 (d, $^1J_{C,P}$ = 105.6 Hz, ^{q}C–P), 34.1 (^{q}C), 31.2 (CH_3) ppm. ^{31}P{^{1}H} NMR (162 MHz, $CDCl_3$): δ 52.8 ppm. HRMS(ESI) *m/z*: calcd for [M+H]: 495.2664, found 495.2649.

[1] M. Korb and H. Lang, *Inorg. Chem. Commun.,* 72 (2016) 30–32.
[2] I. Yu. Kudryavtsev, T. V. Baulina, M. P. Pasechnik, R. R. Aisin, S. V. Matveev, P. V. Petrovskii, and E. E. Nifant´ev, *Russ. Chem. Bull., Int. Ed.,* 62 (2013) 1086–1090.
[3] R.S. Tanke, E. M. Holt and R. H. Crabtree., *Inorg. Chem.,* 30 (1991) 1714-1719.
[4] S. Karagoca, F. Severac, E.-M. Collins, A. Stab, A. Davis, M. Souchet, G. Herve, *J. Haz. Mat.*, 470 (2024) 134236.

II. NMR spectra

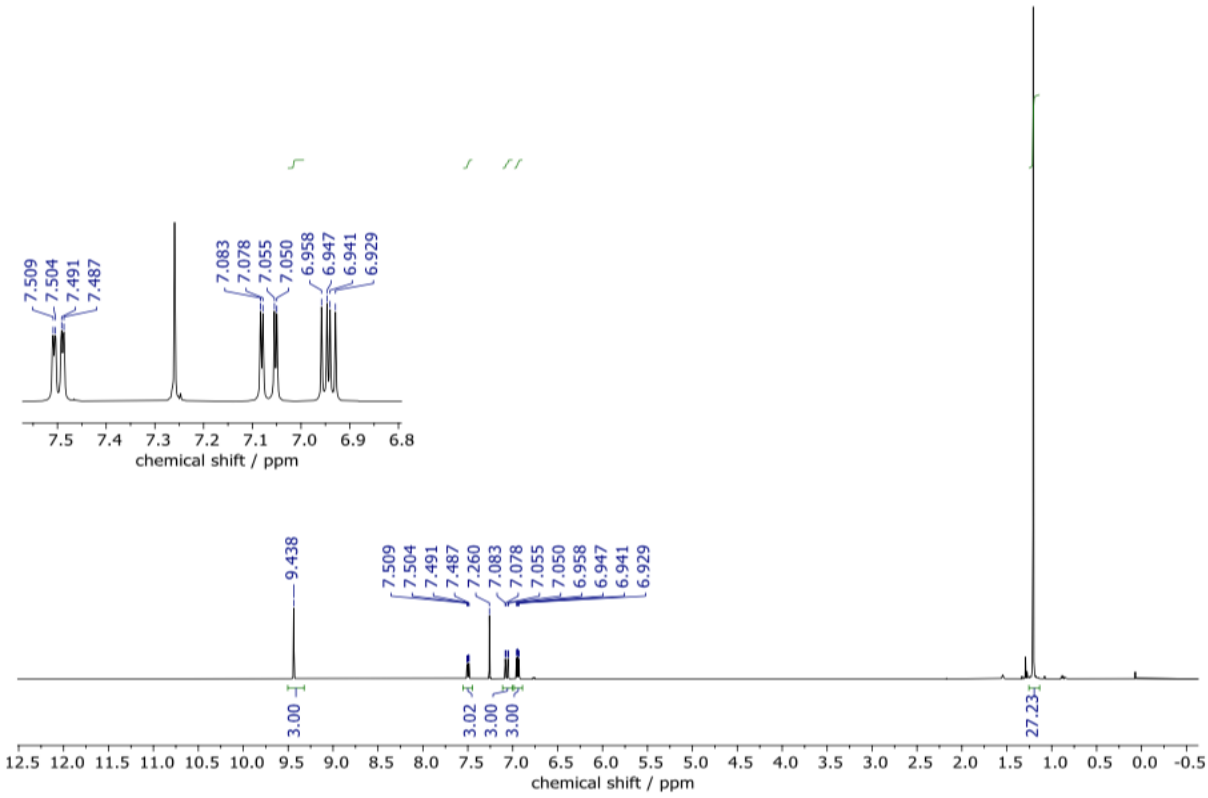

Figure S1: ^{1}H NMR (400 MHz; $CDCl_3$) of **LH_3**.

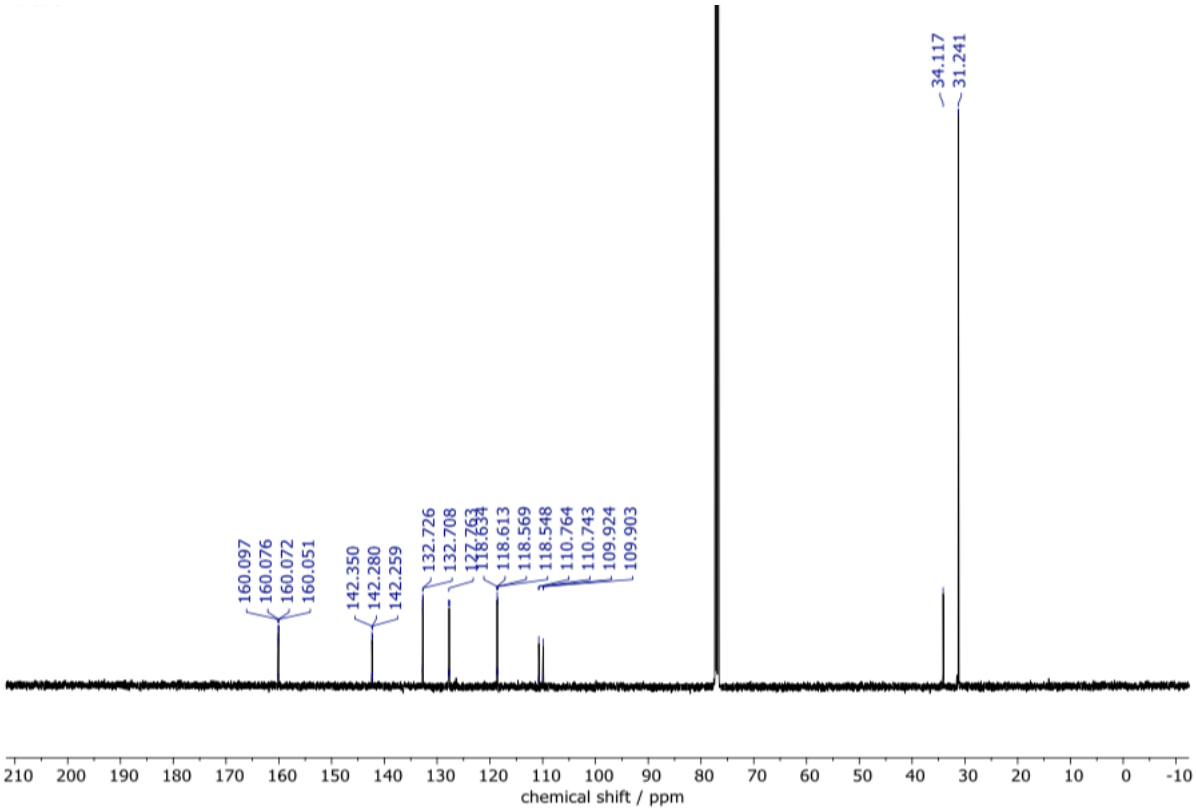

Figure S2: $^{13}C\{^{1}H\}$ NMR (101 MHz, $CDCl_3$) of **LH_3**.

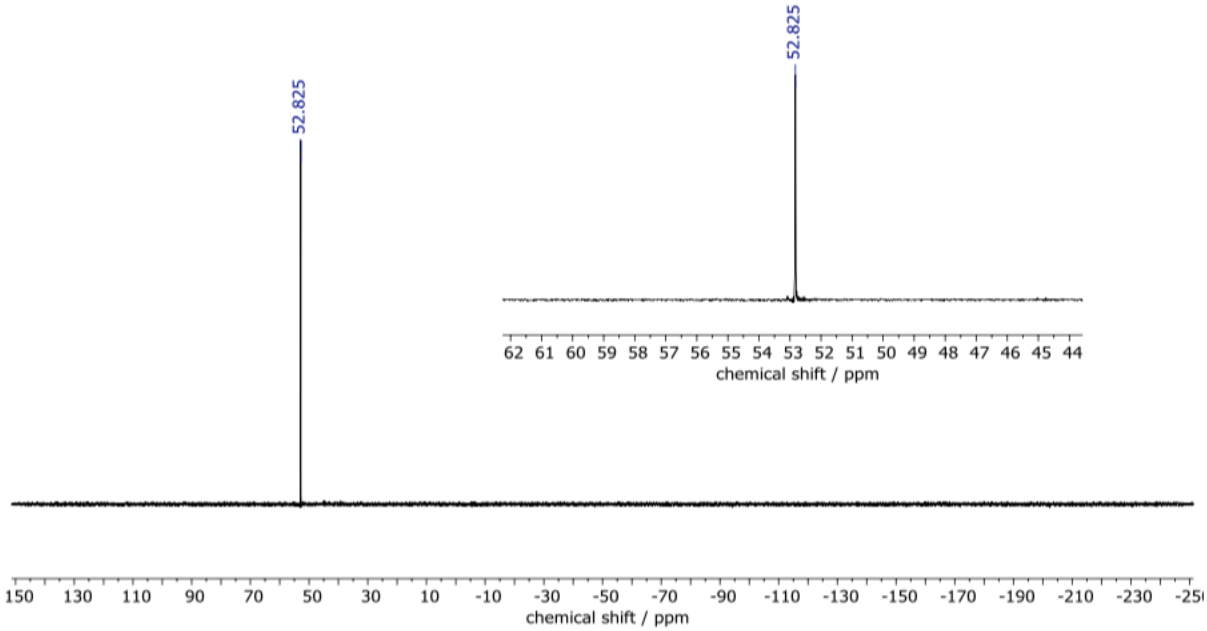

Figure S3: $^{31}P\{^{1}H\}$ NMR (162 MHz, $CDCl_3$) of **LH_3**.

III. Additional Characterisation

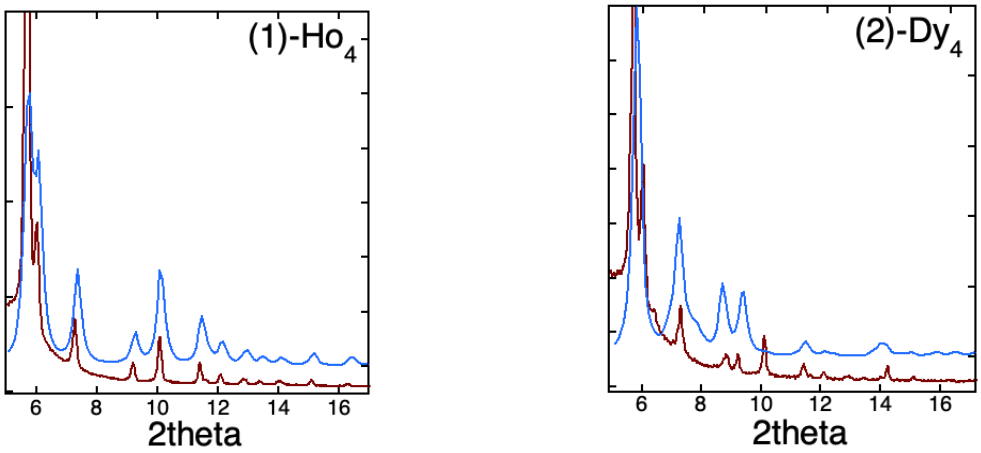

Figure S4: Powder Xray Diffraction pattern (red) along with generated pattern (blue) for complex **1** and **2**. A flat sample holder has been used for collection (~50 mg of ground powder supported by grease) the rotation axis is perpendicular (ϕ scan) to the sample surface.

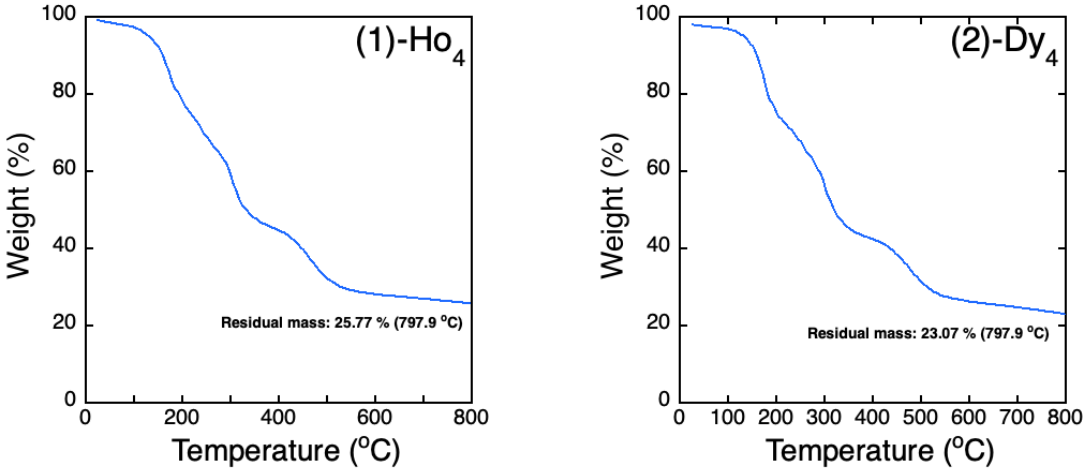

Figure S5a: Thermogravimetric analysis curves (TGA) of bulk crystalline powder used in magnetic studies. Compounds have a similar profile, whereby the curve slowly decreases from 60 as uncoordinated solvent is lost. The complex then has three step decomposition profile. The first step likely from loss of coordinated solvents and a two step decomposition of the ligand follows and the residual mass at 800 °C is consistent with {[Ln(OH)]$_4$} has a calculated mass of ~23 %. The thermal analysis is given below.

	T_{onset} (°C)	T_{max} (°C)	Mass change (-%)
Complex 1			
Lattice Solvent	60.2	120.2	2.45
1	139.8	155.7	9.80
2	295.7	313.9	7.57
3	429.2	472.2	9.05
Complex 2			
Lattice Solvent	60.2	152.2	5.52
1	153.6	169.4	14.02
2	292.9	305.2	7.15
3	440.8	473.6	4.69

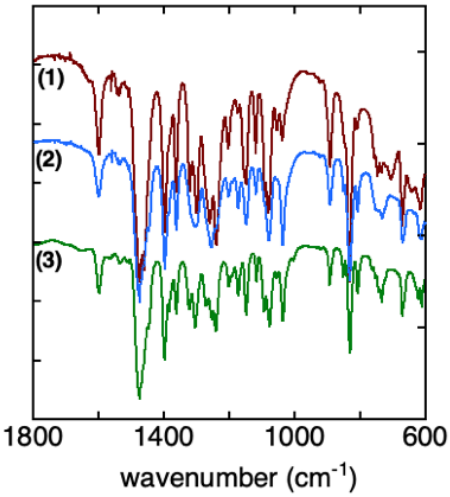

Figure S5b: FTIR-ATR spectrum of complex **1**(red), **2**(blue) and **3**(green).

IV. X-ray Crystallography

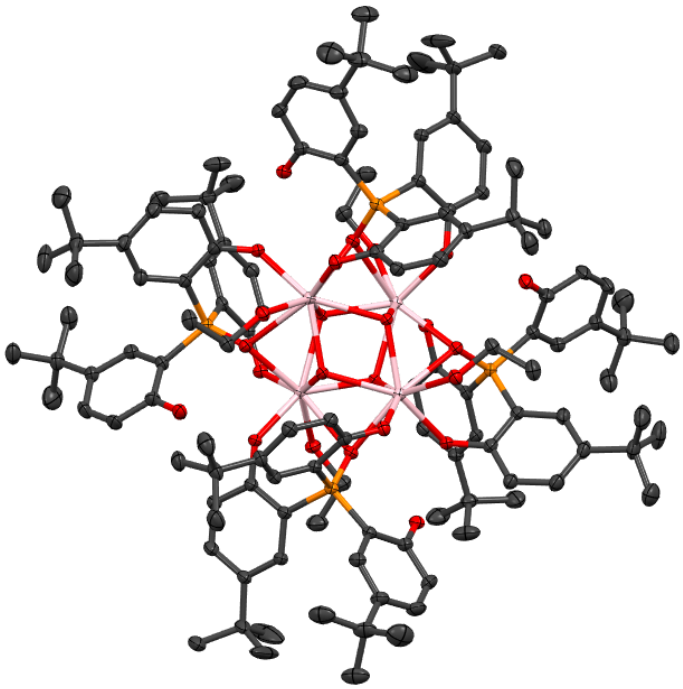

Figure S6: Representation of the structure for complex **1**. Thermal ellipsoids are set to 30 % probability. Hydrogen atoms and solvent molecules have been omitted for clarity. Pink = Ho^{III}, red = O, orange = P and grey = C atom.

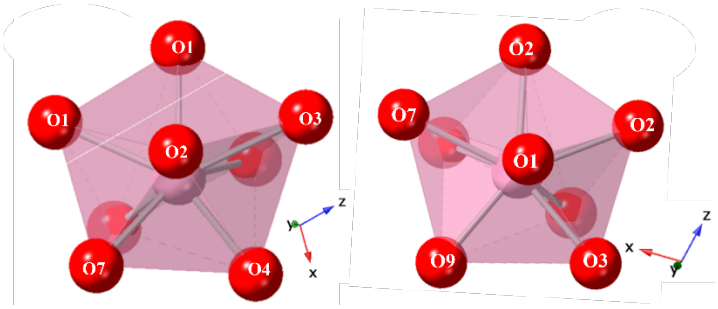

Figure S7: Polyhedral view of the eight-coordinate geometries of Ho in complex **1,** the three μ_3-OH are located above the Ln centre. This depiction from CrystalMaker® v10.8.2 supports the calculated SHAPE deviations [5] for an eight coordinate Ln environment. Pink = Ho^{III} and red = O atom.

Table S1: Selected interatomic distances (Å) and shape parameters for complex **1**.

	Ho1	Ho2
Distances (Å)		
Ho–O1 (μ_3-OH)	2.299(3)	-
Ho–O1 (μ_3-OH)	2.425(3)	2.324(4)
Ho–O2 (μ_3-OH)	2.319(4)	2.300(3)
Ho–O2 (μ_3-OH)	-	2.428(3)
Ho–O3 (P=O)	2.665(4)	2.407(3)
Ho–O4	2.242(3)	-
Ho–O7 (P=O)	2.411(3)	2.638(4)
Ho–O8	2.221(4)	-
Ho–O11 (CH_3CH_2OH)	2.362(4)	-
Ho–O5	-	2.232(4)

Ho–O9	-	2.246(4)
Ho–O12 (CH_3CH_2OH)	-	2.358(4)
Distortion SHAPE		
BTPR-8 *(C_{2v})*	1.445	1.492
TDD-8 *(D_{2d})*	1.570	1.579
JBTP-8 *(C_{2v})*	1.503	1.602
JSD-8 *(D_{2d})*	2.616	2.739
SAPR-8 *(D_{4d})*	2.844	2.850

SHAPE [5] is used to calculate deviation of the Ln centre from idealised polyhedra with continuous shape measure (CShM) with symmetry noted. Acceptable deviations[6] up to 5-10 % are given: Biaugmented trigonal prism (BTPR-8), Trigonal dodecahedron (TDD-8), Johnson-Biaugmented trigonal prism (JBTP-8) Square antiprism (SAPR-8), Snub disphenoid (JSD-8);

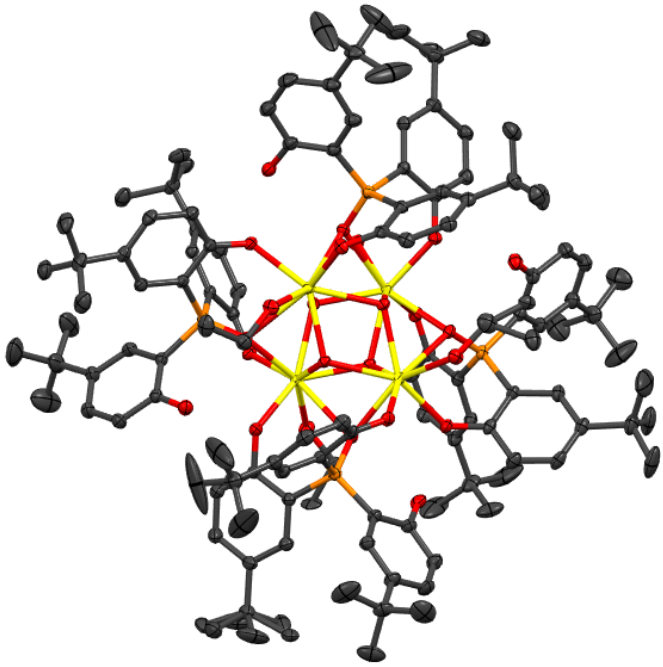

Figure S8: Representation of the structure for complex **2**. Thermal ellipsoids are set to 30 % probability. Hydrogen atoms and solvent molecules have been omitted for clarity. Yellow = Dy^{III}, red = O, orange = P and grey = C atom.

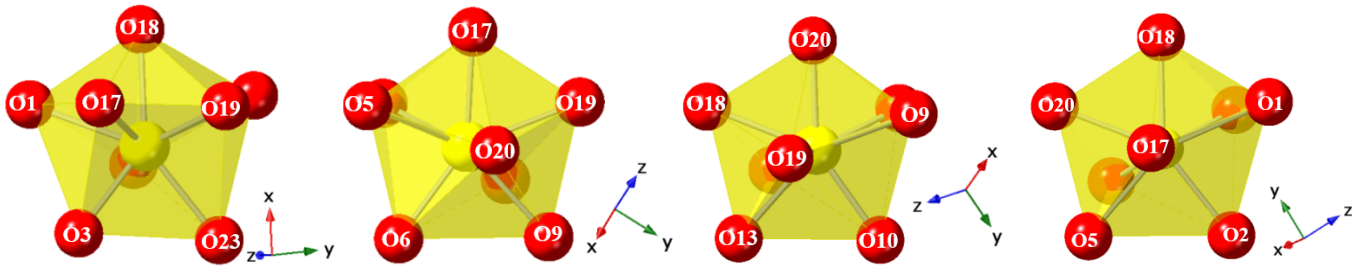

Figure S9: Polyhedral view of the eight-coordinate geometries of Dy in complex **2**, the three μ_3-OH are located above the Ln centre. This depiction from CrystalMaker® v10.8.2 supports the calculated SHAPE deviations [5] for an eight coordinate Ln environment. Yellow = Dy^{III} and red = O atom.

Table S2: Selected interatomic distances (Å) and shape parameters for complex **2**.

	Dy1	Dy2	Dy3	Dy4
Distances (Å)				
Dy–O17 (μ_3-OH)	2.393(3)	2.360(3)	2.336(3)	-
Dy–O18 (μ_3-OH)	2.350(2)	2.321(3)	-	2.379(3)
Dy–O19 (μ_3-OH)	2.324(3)	-	2.384(3)	2.384(2)
Dy–O20 (μ_3-OH)	-	2.374(3)	2.370(2)	2.318(3)
Dy–O23 (CH_3CH_2OH)	2.387(3)	-	-	-
Dy–O13 (P=O)	2.632(3)	-	-	2.414(3)
Dy–O14	2.280(3)	-	-	-
Dy–O3	2.272(3)	-	-	-
Dy–O1 (P=O)	2.450(3)	2.683(3)	-	-
Dy–O7	-	2.277(3)	-	-
Dy–O2	-	2.247(3)	-	-
Dy–O5 (P=O)	-	2.458(3)	2.607(2)	-
Dy–O21 (H_2O)	-	2.348(3)	-	-
Dy–O22 (CH_3CH_2OH)	-	-	2.389(3)	-
Dy–O6	-	-	2.261(3)	-
Dy–O9 (P=O)	-	-	2.449(3)	2.661(3)
Dy–O11	-	-	2.265(3)	-
Dy–O10	-	-	-	2.236(3)
Dy–O15	-	-	-	2.301(3)
Dy–O24 (CH_3CH_2OH)	-	-	-	2.350(3)
Distortion SHAPE				
BTPR-8 *(C_{2v})*	1.352	1.281	1.119	1.369
TDD-8 *(D_{2d})*	1.680	1.867	1.875	1.584
JBTP-8 *(C_{2v})*	1.520	1.308	1.353	1.536
JSD-8 *(D_{2d})*	3.205	3.145	3.296	3.114
SAPR-8 *(D_{4d})*	2.124	2.526	2.127	2.491

SHAPE [5] is used to calculate deviation of the Ln centre from idealised polyhedra with continuous shape measure (CShM) with symmetry noted. Acceptable deviations[6] up to 5-10 % are given: Biaugmented trigonal prism (BTPR-8), Trigonal dodecahedron (TDD-8), Johnson-Biaugmented trigonal prism (JBTP-8) Square antiprism (SAPR-8), Snub disphenoid (JSD-8);

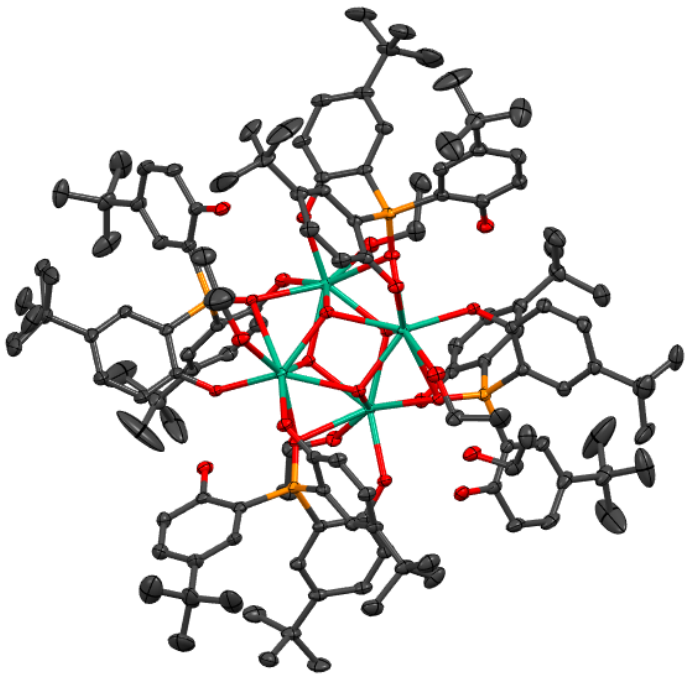

Figure S10: Representation of the structure for complex **3**. Thermal ellipsoids are set to 30 % probability. Hydrogen atoms and solvent molecules have been omitted for clarity. Green = Tb^{III}, red = O, orange = P and grey = C atom.

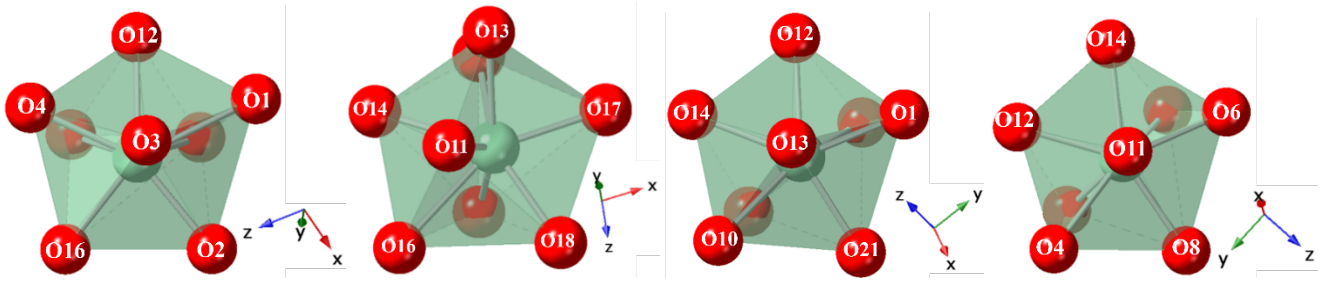

Figure S11: Polyhedral view of the eight-coordinate geometries of Tb in complex **3**, the three μ_3-OH are located above the Ln centre. This depiction from CrystalMaker® v10.8.2 supports the calculated SHAPE deviations [5] for an eight coordinate Ln environment. Green = Tb^{III} and red = O atom.

Table S3: Selected interatomic distances (Å) and shape parameters for complex **3**.

	Tb1	Tb2	Tb3	Tb4
Distances (Å)				
Tb–O11 (μ_3-OH)	2.401(4)	2.328(4)	-	2.359(3)
Tb–O12 (μ_3-OH)	2.388(3)	-	2.402(4)	2.339(4)
Tb–O13 (μ_3-OH)	2.320(4)	2.394(4)	2.379(3)	-
Tb–O14 (μ_3-OH)	-	2.367(3)	2.341(4)	2.410(4)
Tb–O1 (P=O)	2.655(4)	-	2.466(4)	-
Tb–O2 (CH_3CH_2OH)	2.353(5)	-	-	-
Tb–O3	2.258(4)	-	-	-
Tb–O4 (P=O)	2.426(5)	-	-	2.639(4)
Tb–O16	2.314(4)	-	-	-
Tb–O6 (P=O)	-	2.684(5)	-	2.463(4)
Tb–O9	-	2.268(4)	-	-
Tb–O10 (P=O)	-	2.467(4)	2.592(4)	-
Tb–O17	-	2.283(5)	-	-
Tb–O18 (CH_3CH_2OH)	-	2.377(4)	-	-
Tb–O15 (CH_3CH_2OH)	-	-	2.402(4)	-
Tb–O21	-	-	2.279(5)	-
Tb–O32	-	-	2.275(4)	-
Tb–O5	-	-	-	2.276(4)
Tb–O7 (CH_3CH_2OH)	-	-	-	2.395(4)
Tb–O8	-	-	-	2.300(4)
Distortion SHAPE				
BTPR-8 *(C_{2v})*	1.374	1.252	1.131	1.359
TDD-8 *(D_{2d})*	1.599	1.937	1.870	1.709
JBTP-8 *(C_{2v})*	1.585	1.349	1.409	1.545
JSD-8 *(D_{2d})*	3.141	3.183	3.268	3.245
SAPR-8 *(D_{4d})*	2.578	2.563	2.541	2.153

SHAPE [5] is used to calculate deviation of the Ln centre from idealised polyhedra with continuous shape measure (CShM) with symmetry noted. Acceptable deviations[6] up to 5-10 % are given: Biaugmented trigonal prism (BTPR-8), Trigonal dodecahedron (TDD-8), Johnson-Biaugmented trigonal prism (JBTP-8) Square antiprism (SAPR-8), Snub disphenoid (JSD-8);

Table S4: Selected Ln–Ln distances (Å), Ln–O–Ln angles (°), O–Ln–O angles (°) and Ln-Ln-Ln angles (°) in **1, 2** and **3**.

	1	**2**	**3**
Distance (Å)			
Ln1-Ln2	3.549	3.619	3.959
Ln1-Ln3	-	3.968	3.634
Ln1-Ln4	-	3.595	3.613
Ln2-Ln3	-	3.584	3.603
Ln2-Ln4	-	3.931	3.641
Ln3-Ln4	-	3.614	3.994
Angle(°)			
Ln1-O17-Ln2	-	99.20	-
Ln1-O17-Ln3	-	114.11	-
Ln1-O18-Ln2	-	101.59	-
Ln1-O18-Ln4	-	98.95	-
Ln1-O19-Ln3	-	114.86	-
Ln1-O19-Ln4	-	99.54	-
Ln2-O17-Ln3	-	99.52	-
Ln2-O18-Ln4	-	113.54	-
Ln2-O20-Ln3	-	98.15	-
Ln2-O20-Ln4	-	113.81	-
Ln3-O19-Ln4	-	98.56	-
Ln3-O20-Ln4	-	100.98	-
Ln1-O1-Ln2	96.72	-	-
Ln1-O2-Ln2	100.43	-	-
Ln1-O7-Ln2	89.23	-	-
Ln1-O1-Ln1′	114.40	-	-
Ln1-O2-Ln2′	97.05	-	-
Ln1-O3-Ln2′	88.92	-	-
Ln2-O2-Ln2′	114.96	-	-
Ln1-O1-Ln2′	100.63	-	-
Ln1-O11-Ln2	-	-	113.71
Ln1-O11-Ln4	-	-	98.77
Ln1-O12-Ln3	-	-	98.70
Ln1-O12-Ln4	-	-	99.71
Ln1-O13-Ln2	-	-	114.25
Ln1-O13-Ln3	-	-	101.30
Ln2-O11-Ln4	-	-	101.93
Ln2-O13-Ln3	-	-	98.02
Ln2-O14-Ln3	-	-	99.88
Ln2-O14-Ln4	-	-	99.32
Ln3-O12-Ln4	-	-	114.82
Ln3-O14-Ln4	-	-	114.43
Ln1-Ln2-Ln3	-	66.85	57.21
Ln1-Ln2-Ln4	-	56.68	57.59
Ln1-Ln3-Ln4	-	56.37	56.30
Ln1-Ln3-Ln2	-	57.00	66.33
Ln1-Ln4-Ln2	-	57.28	66.16
Ln1-Ln4-Ln3	-	66.80	56.80
Ln2-Ln3-Ln4	-	66.20	56.98
Ln2-Ln4-Ln3	-	56.54	56.09
Ln2-Ln1-Ln3	-	56.15	56.47
Ln2-Ln1-Ln4	-	66.04	57.25
Ln3-Ln1-Ln4	-	56.84	66.89
Ln3-Ln2-Ln4	-	57.26	66.92
O1-Ln1-O1	65.57	-	-
O1-Ln1-O2	74.74	-	-
O1-Ln1-O2	77.10	-	-
O2-Ln2-O2	65.10	-	-
O1-Ln2-O2	77.05	-	-
O1-Ln2-O2	74.49	-	-
O17-Ln1-O18	-	74.31	-
O17-Ln1-O19	-	65.54	-

O18-Ln1-O19	-	76.17	-
O17-Ln2-O18	-	75.47	-
O17-Ln2-O20	-	75.58	-
O18-Ln2-O20	-	66.33	-
O17-Ln3-O19	-	65.49	-
O17-Ln3-O20	-	76.12	-
O19-Ln3-O20	-	74.95	-
O18-Ln4-O19	-	74.50	-
O18-Ln4-O20	-	66.30	-
O19-Ln4-O20	-	75.90	-
O11-Ln1-O12	-	-	74.37
O11-Ln1-O13	-	-	66.02
O12-Ln1-O13	-	-	75.79
O11-Ln2-O13	-	-	65.99
O11-Ln2-O14	-	-	75.26
O13-Ln2-O14	-	-	75.13
O12-Ln3-O13	-	-	74.43
O12-Ln3-O14	-	-	65.41
O13-Ln3-O14	-	-	75.89
O11-Ln4-O12	-	-	76.10
O11-Ln4-O14	-	-	73.90
O12-Ln4-O14	-	-	65.34

[5] M. Llunell, D. Casanova, J. Cirera, P. Alemany, S. Alvarez, *SHAPE Program version 2.0* Universitat de Barcelona, Barcelona, Spain, 2010.
[6] S. Alvarez *Dalton Trans.,* 50 (2021) 17101-17119

Table S5: Single crystal X-ray crystallographic data for **1–3**. ~1 month

	1	**2**	**3**
CCDC	2491822	2491821	2491820
M	Ho	Dy	Tb
Empirical formula	$C_{128}H_{176}Ho_4O_{24}P_4$	$C_{60}H_{60}Dy_4OP_4$	$C_{136}H_{201.60}O_{28.80}P_4Tb_4$
Formula weight	2882.28	1570.96	3056.92
Temperature	99.98(10)	100(2)	100.00(10)
λ / Å	1.54184	1.54184	1.54184
space group	*C*2/*c*	$P2_1/c$	$P2_1/c$
Crystal System	monoclinic	monoclinic	monoclinic
a / Å	36.6346(6)	15.42910(10)	15.39750(10)
b / Å	10.5685(2)	35.2632(3)	35.3854(3)
c / Å	34.5274(6)	28.8975(3)	28.9254(2)
α / °	90	90	90
β / °	103.025(2)	98.7970(10)	98.7870(10)
γ / °	90	90	90
V / Å^3	13024.1(4)	15537.6(2)	15574.9(2)
ρ / Mg m^{-3}	1.47	0.672	1.304
Z	4	4	4
Abs coeff / mm^{-1}	5.321	10.608	9.642
F(000)	5856	3008	6272
Crystal size / mm	0.125·0.073·0.053	0.170·0.090·0.030	0.214·0.111·0.028
θ range / deg	2.627 to 66.494 deg.	2.898 to 75.937 deg.	2.904 to 66.499 deg.
Limiting indices	$-43\le h\le 43$ $-12\le k\le 10$ $-40\le l\le 41$	$-19\le h\le 18$ $-43\le k\le 44$ $-29\le l\le 36$	$-18\le h\le 18$ $-42\le k\le 42$ $-32\le l\le 34$
Reflections collected / unique	90414 / 11463	205206 / 31358	223575 / 27407
R_{int}	0.0767	0.079	0.0897
Completeness to θ	99.80%	99.90%	99.80%
Abs. correction	Gaussian	Gaussian	Gaussian
Max. / min. transmit.	1.000 and 0.928	N/A	1.000 and 0.661
Refinement method	Full-matrix least-squares on F^2	Full-matrix least-squares on F^2	Full-matrix least-squares on F^2
Data / restr / param	11463 / 0 / 723	31358 / 0 / 1564	27407 / 1782 / 1607
G.o.o.f on F^2	1.027	0.961	1.034
Final R indices [I>2sigma(I)]	$R1$ = 0.0562, $wR2$ = 0.1551	$R1$ = 0.0530, $wR2$ = 0.1406	$R1$ = 0.0572, $wR2$ = 0.1476
R indices (all data)	$R1$ = 0.0682, $wR2$ = 0.1611	$R1$ = 0.0706, $wR2$ = 0.1539	$R1$ = 0.0663, $wR2$ = 0.1519
Large peak / hole / e A^{-3}	1.397 and -0.957	1.089 and -1.659	2.605 and -1.256

V. Magnetic Measurements

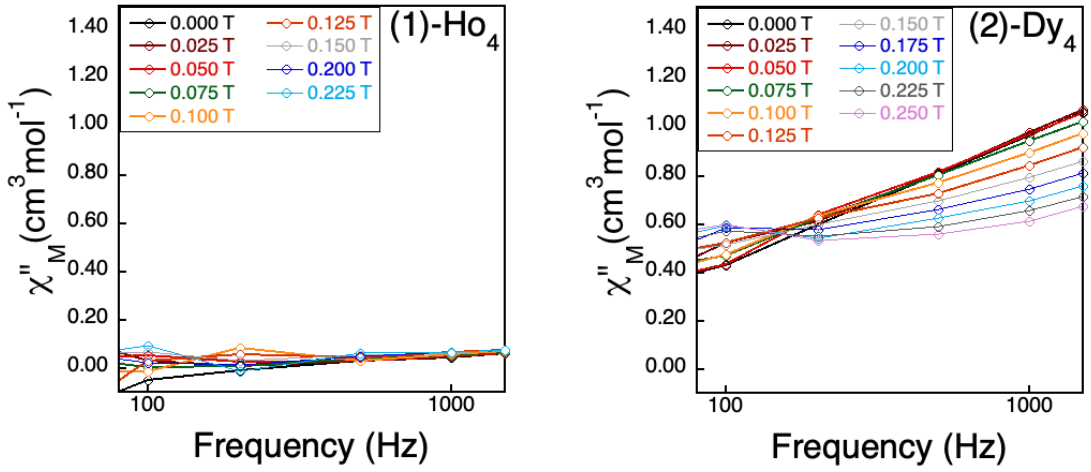

Figure S12: Frequency and field dependent out-of-phase AC susceptibility for **1** and **2** at 2.7 K.

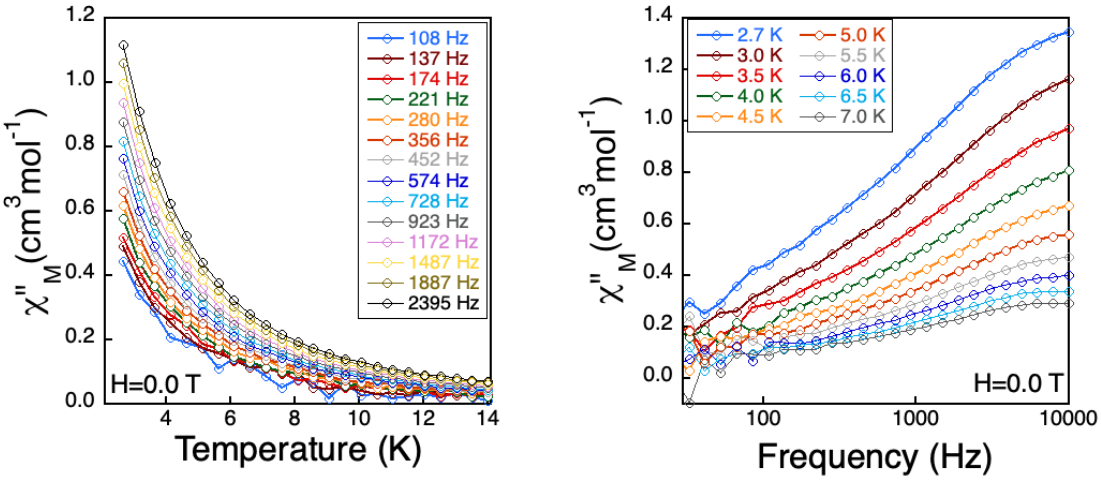

Figure S13: Temperature dependent out-of-phase AC susceptibility in 0 T DC applied field for complex **2**.

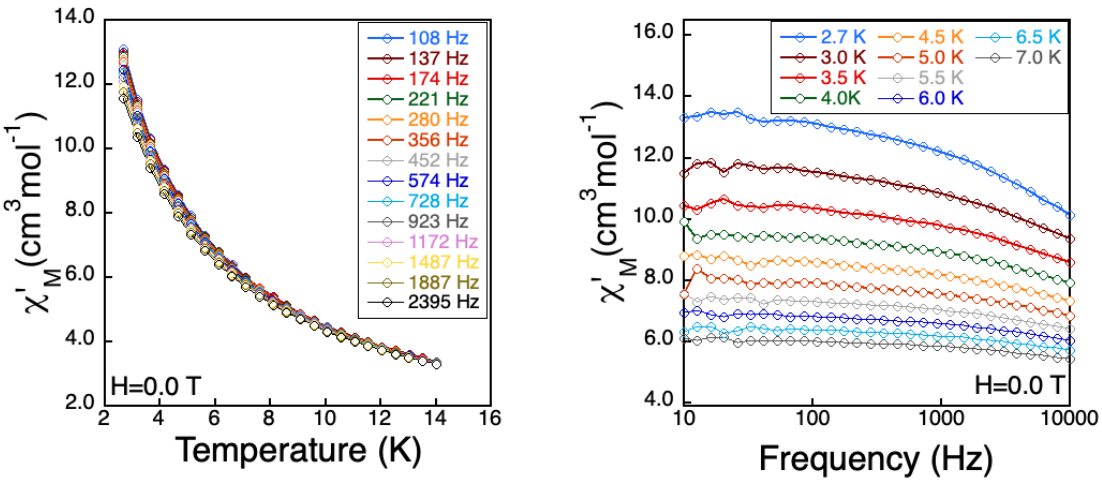

Figure S14: Temperature dependent in-phase AC susceptibility in 0 T DC applied field for complex **2**.